ANAS Transactions **Earth Sciences** **2 / 2024**

http://www.journalesgia.com

LANDSLIDE MODELING USING GIS AND A STATISTICAL METHOD UPSTREAM OF PORT TANGIER MED (TANGIER, MOROCCO)

Maktite A., Faleh A.

Faculty of Letters and Human Sciences, Saïs-Fès, Department of Geography, Sidi Mohammed ben Abdellah University, Fès, Morocco: maktiteabderrahim@gmail.com, ali.faleh@usmba.ac.ma

Keywords: *port, Mediterranean Tangier, informative value, success curves, forecast curves*

Summary. The context of this study is crucial for understanding the challenges faced by the Tanger Med Port, a strategic hub for international trade. Located in a mountainous region, this port is particularly vulnerable to natural hazards, especially landslides. A study conducted on a 193 km² test site recorded 277 slope movements, representing about 11% of the total area. This evaluation of terrain susceptibility used the information value method to map the movements over recent decades as well as six predisposing factors.

The results show that nearly 31% of the total area is highly susceptible to mass movements, 22% is very sensitive, and 23.3% presents a low threat. These findings were rigorously compared and validated using success rate and prediction rate curves. Five major risk classes for landslides were identified in areas that are undeveloped or sparsely developed with low to negligible values and developed areas on mountain slopes with very high-risk values.

Accurate mapping and risk analysis are essential for developing management and prevention strategies to minimize potential impacts on port infrastructure and associated economic activities. This study thus contributes to a better understanding of geological risks in the region and more importantly, to the implementation of appropriate measures to ensure the safety and resilience of the port.

Introduction

The mountains of the Moroccan Rif are subject to instabilities, often in the form of mass movements, which can have a direct impact on urban constructions (Flageollet, 1989; Maate, 1996). These instabilities are caused by various factors, such as an aggressive climate, rugged terrain, the presence of soft ground (such as marl and flysch), as well as aggravating anthropogenic factors. In the Ksar-Sghir area, for example, several landslides have caused varying degrees of damage to the urban area, including the destruction of some houses and the temporary closure of important roads, leading to major disruptions in road traffic. However, the loss of human life associated with these phenomena has always been rare in this region. To deal with these problems, the Directorate of Equipment and Transport allocates about 50% of its annual budget to either strengthen or repair the roads and hydraulic infrastructures damaged by landslides, according to a source from MATEE. In 2005, however, these unforeseen events caused significant economic losses on a national scale and compromised the development of the region.

It is therefore essential to study and map the risks of mass movements in order to implement preventive actions against these complex phenomena. This is why the establishment of landslide risk maps is of crucial importance. Indeed, the United Nations Office for Natural Disaster Reduction (UNDRO, 1979) was the first international institution to emphasize the importance of this type of cartographic documents for estimating the risks associated with a natural phenomenon in particular. Later, during the "International Decade for the Prevention of Natural Disasters" (DIPCN) in Paris in 1999, the usefulness of hazard maps for the prevention of natural disasters and the management of the territory was reaffirmed (El Kharim, 2002). In Morocco, the only documents drawn up so far relating to the hazard linked to landslides have been:

a. the hazard map of the movements of the slopes of the Rif at the scale of 1/1000000 drawn up by Milliés-Lacroix in 1968
b. the mapping work landslide risks in the Taounate region carried out by Avenard in 1965 and Fares in 1994
c. the landslide risk mapping trial in the Al Hoceima region carried out by Margaa in 1994, landslide risk mapping in the Tetouan region drawn up by El Kharim in 2002 and the mapping

of the hazard linked to landslides in the Tangier peninsula carried out by Sossey Alaoui in 2005 and Faleh et al. in 2002.

Initially, researchers faced the difficulty of superimposing and analyzing geographical information that varies in time and space. However, the emergence of Geographic Information Systems (GIS) and the development of computer science have made it possible to carry out complex spatial analyses. This made it possible to analyze geographic information, apply particular algorithms, perform statistical analyses and model the results. Several researchers have underlined the importance of this approach for mapping the hazard associated with landslides (Brabb, 1984, 1987; Wadge, 1988; van Westen et al., 1993; Brabb, 1995; Carrara et al., 1995; Irigaray, 1995; Soeters and Van Westen, 1996; El Kharim, 2002; Maquaire and Ambrose, 2002). Furthermore, some researchers have highlighted the interest of combining satellite imagery with GIS to establish maps of the hazard linked to landslides (Rouzeau and Scanvic, 1992; Leroi et al., 1992; van Westen, 1993).

As part of our study, we mapped the risk associated with landslides in order to benefit from precise knowledge of this phenomenon in the region studied. This detailed cartographic representation is all the more justified as human activity in these areas is becoming increasingly intense. Our work is therefore divided into several stages:

– Listing the slope movements described in the bibliography.

– Understanding their distribution by identifying predisposing and triggering factors.

– Mapping each factor contributing to the genesis of mass movements (predictive factors).

– Determining the areas impacted by these phenomena, as well as the infrastructure, equipment and vulnerable populations.

– Developing a representation of the risk of landslides in order to prevent hazards by integrating the data into a GIS.

I. Presentation of the Study Area

The study area extends over an area of 193 km² and is located upstream of the Mediterranean port complex of Tangier, in the Tangier peninsula in northwestern Morocco. It encompasses the three basins of Oued R'mel, Oued Ksar Sghir and Oued Ghlala (Fig.1).

The geomorphological characteristics of this area include slopes which are rather steepy as well as a very rugged mountainous relief composed of mountains and valleys extending from East to West.

From a geological point of view, the study region is composed of several distinct formations: the Internal Domain, including the Ghomaride and the Limestone Dorsal, the External Domain, including the Internal Tangier Unit and the External Tangier Unit, as well as the flysch nappes, which include the Predorsalian Unit, the Tisirène Beni Ider Unit and the Numidian facies sandstone Unit (Fofana, 2009). The climate in this area is of the subhumid type, with annual rainfall varying between 800 and 1000 mm and average annual temperatures ranging from 17 to 20°C. The main studied rivers in the region are Oued Ksar Sghir, Oued Rhlâlâ and Oued Rmel.

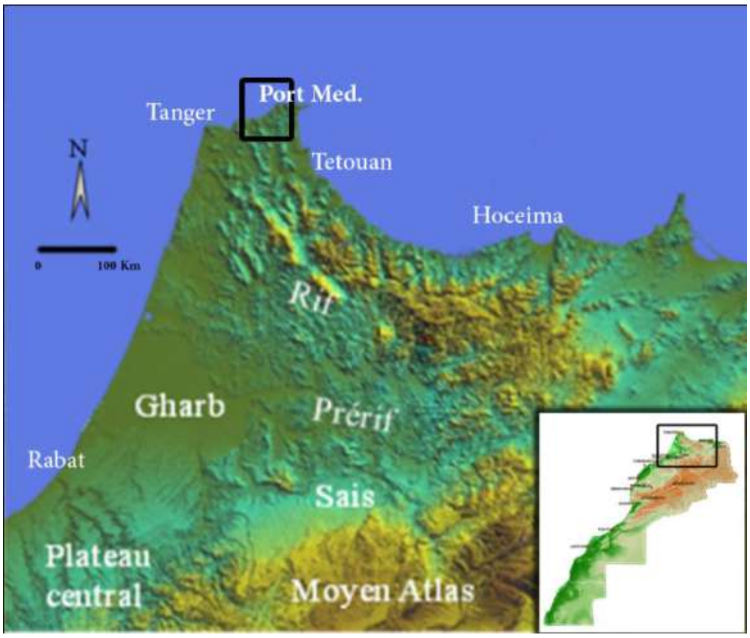

Source: Google Earth Image
Directed by: Maktite Abderrahim

Fig. 1. Location of the studied area

II. Methodology

The method adopted to carry out this study is the method of informative values (VI). It is a statistical method used to assess the forecasting quality of a forecasting model. It measures the ability of a model to correctly predict the actual value of a target variable. The VI is defined as the sum of the absolute differences between the predicted values and the actual values weighed by the relative importance of each target variable. However, the lower the value of the VI, the more accurate the model is considered.

The method is then based on the creation of a risk index map using variable maps, maps of the probability of occurrence of landslides, and maps of the vulnerability of the area studied according to the following steps (Fig. 2):

A. The landslide Hazard

The criteria taken into account to assess landslides generally include their area, speed, depth and the volume of soil displaced. The propensity of lands to undergo landslides is determined by their physical characteristics such as slopes, aspect, concavity, and other factors related to their stability. In addition, the probability of occurrence is used to estimate the risk of landslide in each specific area over a given period.

The process of creating the hazard map involves two steps: on the one hand, the determination of the predisposition of the land to instability (susceptibility), taking into account their physical characteristics (slope, exposure, concavity, etc.) and, on the other hand, the determination of the temporal probability that a given area will experience a landslide in a given period of time.

1. Landslide Inventory

In order to measure the propensity of land to landslides, it is important to identify the areas that have been affected in the past and to observe the characteristics of the affected land. The susceptibility maps that are typically created by the adopted method are based on the idea that future landslides will occur under conditions similar to those that caused previous landslides (Hansen, 1984).

To create a landslide inventory, aerial photo interpretation is usually used for confirmation by fieldwork. This method is considered the best tool for identifying landslides. In this study, we have established the inventory of landslides based on aerial images from Google Earth pro and work already carried out in the region.

2. Predisposing Factors

The method adopted to assess the susceptibility of land in this study area is based on a statistical approach called "Informative Values Method" (VI). This method was chosen because of its objectivity and easy reproducibility. Its fundamental principle is to collect data on the characteristics of the land where landslides have already occurred in order to assess their susceptibility to landslides.

To construct the susceptibility map, six variables were identified using all the data available on the land in the study area, as well as information extracted from the digital terrain model (DTM). These variables are presented in Fig. 4. This data collection allowed us to establish a complete list of the characteristics of the lands; characteristics which were then used to evaluate those lands' susceptibility to landslides.

3. Evaluation and Production of the Susceptibility Map

The informative value of a class in a variable is determined according to the number of landslides that have occurred on lands with the same characteristics as the considered class. More specifically, it is obtained by comparing the number of landslides occurring on the lands of the class to the proportion of lands of this class over the total area studied according to the following formula:

$$\boldsymbol{VI(i) = Ln\left(\frac{Si/Ni}{S/N}\right)} \quad (1)$$

Si: the area of class i slipped
Ni: the area of class i
S: the total area that slipped
N: the total area of the studied area

Once the informative value of each class of each variable has been determined, they are combined to produce an estimate of the overall susceptibility of the terrain in the area. The combination of the informative values is generally carried out using a mathematical model which takes into account the relative importance of each variable in the generation of landslides.

In the Raster representation, each pixel of each variable has a VI value. To create the susceptibility map, these VI values of each variable present in each pixel are summed up and then grouped into different classes.

4. Construction of Success and Forecast Curves

The accuracy of this model is assessed using hit and prediction rates, as defined by Yin and Yan in 1988; Chung and Fabbri in 2003 and cited by Zêzere et al., 2004. The hit rate measures the reliability of the model using the slips that were used to build it. It makes it possible to determine the extent to which the model is capable of correctly reproducing the slips already observed.

The prediction rate, on the other hand, is calculated by introducing part of the slippage into the model and comparing the results obtained with the success and prediction curves. This step verifies the ability of the model to accurately predict landslides based on the characteristics of the terrain.

The analysis of the success and prediction curves, as well as the measurement of the areas under these curves, make it possible to determine the accuracy of the model developed. The more the curves overlap and the larger the areas under the curves, the more accurate the model is considered to be in its ability to assess the susceptibility of the land to landslides.

The analysis of the accuracy of the model is an important aspect to assess the reliability of the susceptibility map obtained. The success and prediction rates provide a measure of the correspondence between the actual slip zones and the slip zones predicted by the model. If the success and prediction rates are high, it means that the model is well adjusted to the real data and can therefore be used with good confidence to predict landslide risk areas in the future. However, if the rates are low, it means the model needs to be improved by using additional variables or changing the methodology used to build the model.

B. The definition of Temporal Probability

The frequency at which the phenomenon occurs is measured by the temporal occurrence probability component of the hazard. To calculate this component, we generally use the recurrence period of the cause that triggered the landslide. In the case of the landslides that have occurred in northern Morocco over the past fifty years, the main cause is heavy rainfall.

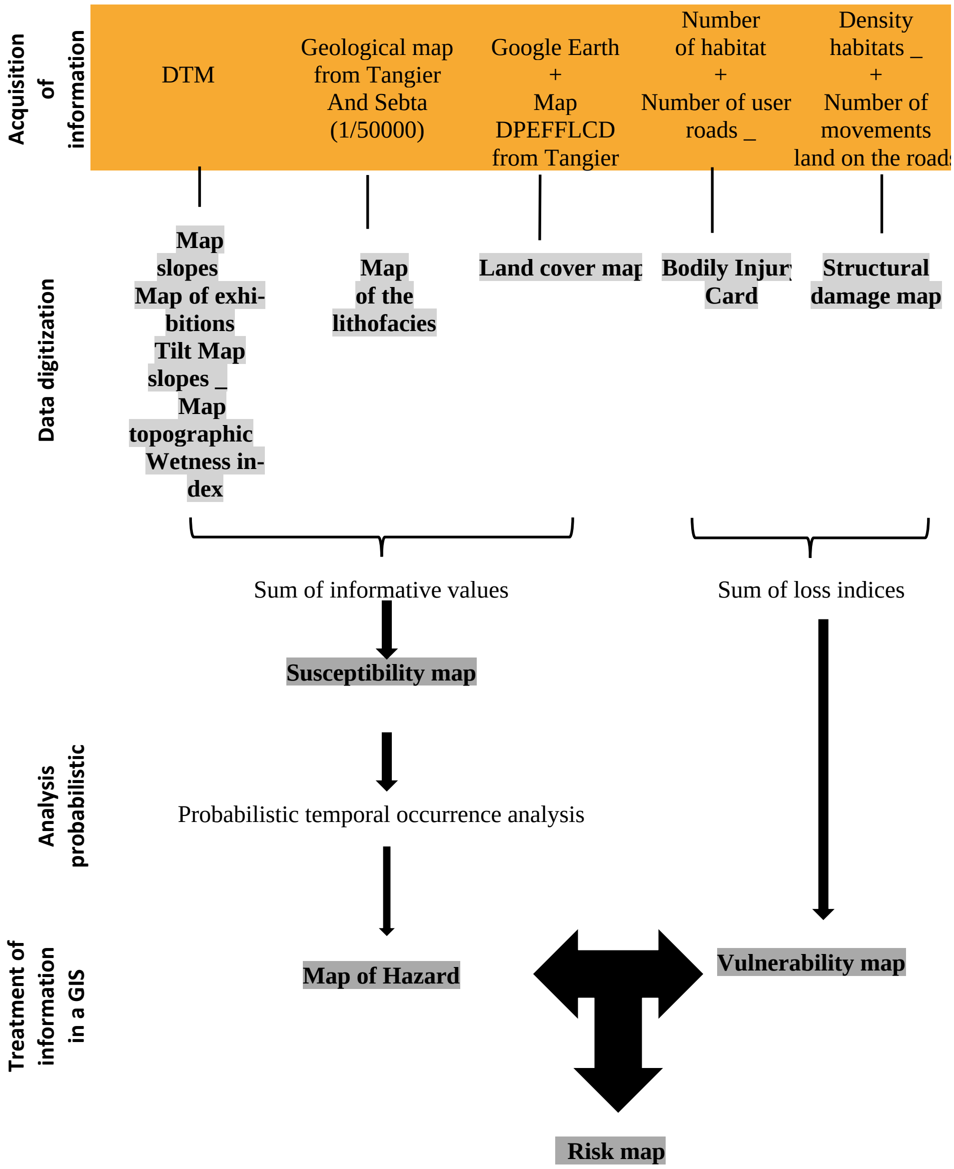

Source: Description of the method
Directed by: Maktite Abderrahim

Fig. 2. Methodological scheme

To estimate the probability of temporal occurrence of landslides, the most common rainfall scenarios that have caused landslides since the 1980s have been identified. It is assumed that the same rains will produce the same types of landslides and will affect the same surfaces. Using formula (2), the probability of temporal occurrence is determined for each landslide susceptibility class.

$$\mathbf{Pi} = \mathbf{1\text{-}(1\text{-}}\frac{\boldsymbol{T\ affectée}}{\boldsymbol{Ti}} * \mathbf{Pr}) \qquad (2)$$

Pi: the probability of the susceptibility class
T affected: the total area of the area that will slip
Ti: the area of the susceptibility class i
Pr: the predictive value of the susceptibility class i

The temporal probability values are determined by the calculations performed to measure the susceptibility, which will be described in detail in the results part. The predictive value, on the other hand, measures the model's ability to predict the location of future landslides based on past landslides.

C. Vulnerability Assessment

To quantify vulnerability, an index is used that takes into account two major criteria: bodily injury and structural damage (Leone, 1996).

- The personal injury assessment includes two factors: the number of inhabitants in the different regions of the study area and the number of vehicles using the different roads in the study area (Fig. 10).
- Structural damage is assessed by taking into account two factors: the population density of each Douar and the number of landslides affecting each road (Fig. 11).

Each pixel in each theme is assigned a value between 0 and 1 based on the loss index. The maximum loss index value is set at 1. Generally, the value 1 is attributed to the most vulnerable class, then the other values are attributed according to this one.

D. Realization of the Risk Map:

Finally, we produced the risk map by superimposing the hazard map with the vulnerability map and based on a matrix that determines the risk classes (Table 1).

The levels of hazard and vulnerability were divided into four classes using quantiles. By crossing these classes, the level of risk was determined.

III. Results and Discussions:

A. Landslide Hazard Map

1. Inventory of Landslides

Before proceeding with the elaboration of the susceptibility map, a preliminary step was carried out. It consisted of an inventory of ground instabilities based on several sources. First, the work of El Gharbaoui B., produced in 1981 were consulted, in particular its geomorphological map of the Tangier peninsula at scale 1/100,000. In addition, the geological maps of the Ministry of Energy and Mines (MEM) at scale 1 /50,000 of Ksar Sghir and Sebta were examined.

In addition to these sources, information from the landslide map produced by Fonseca André Filipe in 2014 was used. This work, which constituted a doctoral thesis entitled "Large deep-seated landslides in the northern Rif Mountains (Northern Morocco): inventory and analysis", provided a valuable contribution to our study. Digital images from Google Earth Pro were also used to complete our information.

Then, field observations were carried out in order to complete and validate the data collected. This step made it possible to obtain additional information and to check the consistency of the data obtained from the various sources mentioned above.

In this way, 277 landslides were identified, of which 38.6% were debris screes, 16% were solifluctions, 23% were mudslides and 22.4% were complex movements (Table 2).

Table 1

Matrix determining the risk classes

		Hazard			
	×	Very weak (Class 1)	Weak (Class 2)	Strong (Class 3)	Very strong (Class 4)
Vulnerability	Very weak (Class 1)	2	3	4	5
	Weak (Class 2)	3	4	5	6
	Strong (Class 3)	4	5	6	7
	Very strong (Class 4)	5	6	7	8

acceptable risk | **Medium high risk** | **High risk**

Table 2

Distribution of landslides in the study area

Type of slips	Number of elaborate slips of: Map by André Filipe, 2014	Geomorphological and geological map	Image from Google Earth	The sum	The surface in (m²)
Complex movements	3	7	52	62	2623700
Mudslides	1	0	63	64	748700
Solifluction	11	16	17	44	8519100
Landslide	4	82	21	107	10082300
Sum	19	105	153	277	21973800

Directed by: Maktite Abderrahim

The landslides identified are aligned in a North-South direction and are distributed around the watercourses of the study area. The number of landslides recorded decreases slightly from northeast to south-west, as shown in Fig. 3.

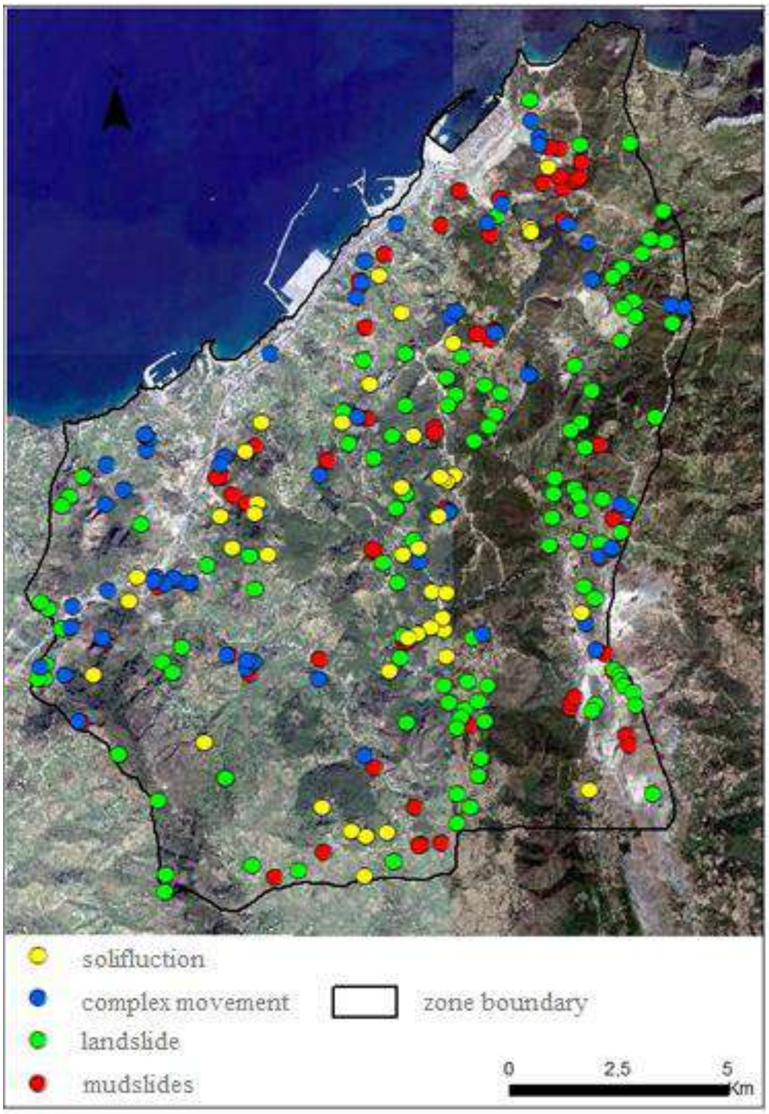

Source: Satellite Image 2016
Directed by: Maktite Abderrahim

Fig. 3. Inventory and location of landslides in the study area

2. Predisposing Factors

Then, it is necessary to list the variables or predisposition factors of the lands that have undergone landslides. Some of these factors come from a digital terrain model (DTM) of the studied area, obtained by digitizing contour lines from 1/25000 topographic maps.

The DTM (Digital Terrain Model) of the study area was created using a pixel size of ten meters on a side. This resolution was determined based on the contour spacing available for building the DEM. Moreover, this pixel size was considered as an appropriate compromise between data precision and the amount of data generated, considering the size of the studied area which is 193 km². Thus, the DEM consists of 1,930,000 pixels, with each pixel representing an area of 100 m².

In the context of this study, the pixel size chosen for each theme is also ten meters per side, with the exception of the concavity/convexity of the slopes. For this variable, the precision of the DEM has been reduced and the pixel size has been increased to 50 meters per side to better represent this specific topographic feature.

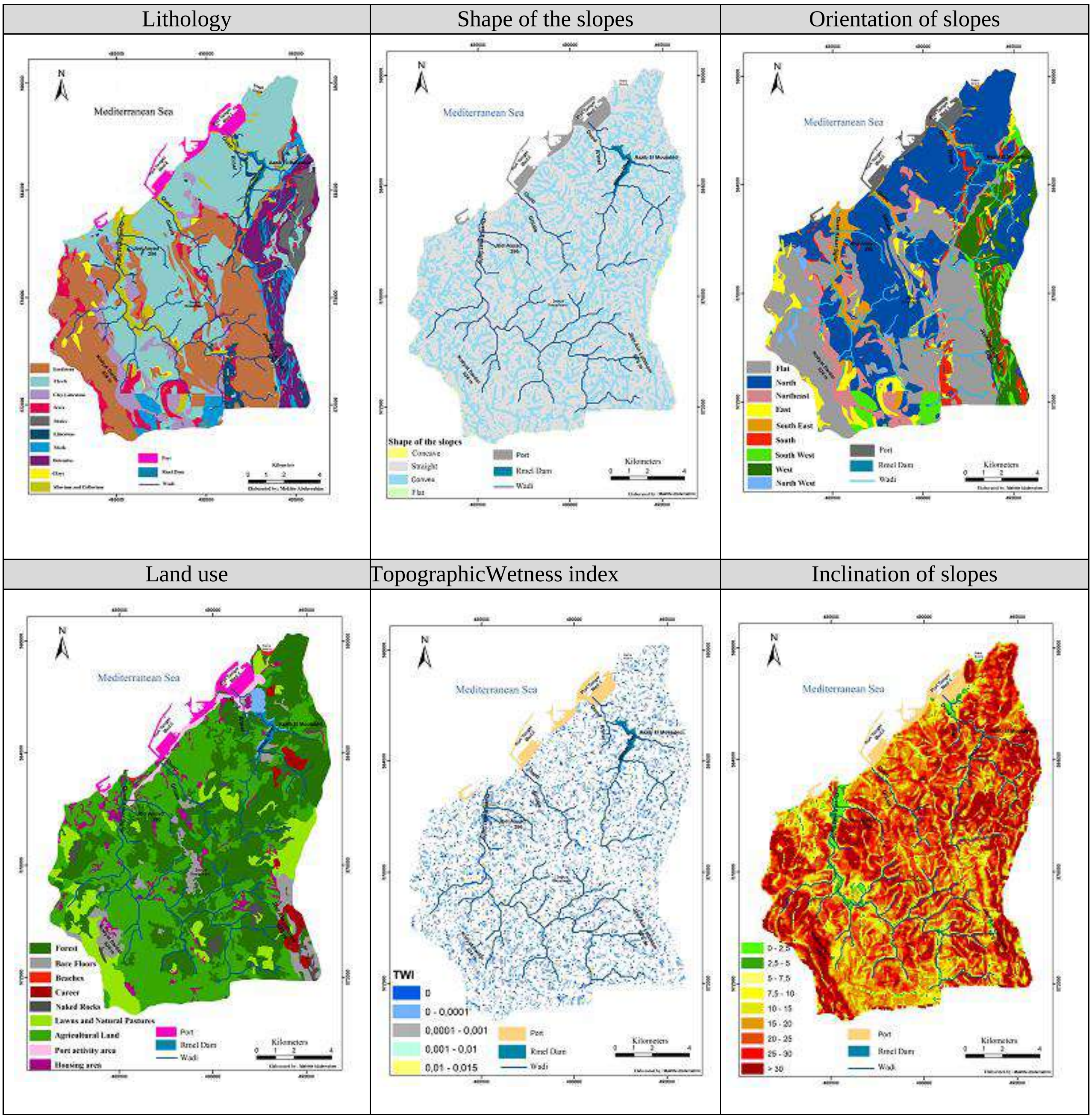

Source: - DTM (1/25000)
-IFN (2014)

Fig. 4. Predisposing factors for susceptibility assessment

With regard to topography Wetness Index (TWI), this is an index used to assess the presence of water in soils and areas of external saturation. For each pixel, this index is calculated according to the following formula:

$$TWI = \boldsymbol{In}(\boldsymbol{A}/\tan \boldsymbol{B})$$

A: Flow Accumulation
B: slope

Using GIS, we were able to determine the number of suspected landslides as well as the total area of each landslide for each of the six themes. We also calculated the informative values for each class using a specific formula (equation 1). For each class of each theme, we measured the area affected by the slip by counting the number of pixels of this class containing a slip point. It should be noted that the slips were represented by dots in this study, with only one slip dot typically present per pixel. Although it is a simplification of reality, this model produced excellent results even if it does not allow an accurate estimation of the volume of earth displaced by a landslide, which would require an evaluation in the field.

The susceptibility is represented by the average value of the VI of each class present in each theme, calculated for each pixel (Dai et al., 2002). However, it is necessary to prove the robustness of this model by evaluating it using the methods of success rate and prediction rate.

3. Evaluation and Production of the Susceptibility Map

Fig. 8 presents the future slip probability for each pixel. The informative values, which reflect the probabilities of the different classes, are divided into "quantiles", in such a way that each class contains the same number of pixels. Classes are defined as follows:

- Class 1 includes the lowest values, located between -5.3348 and 1.1242.
- Class 2 includes values ranging from 1.1243 to 2.4187.
- Class 3 includes values between 2.4188 and 3.8052.
- Finally, class 4 corresponds to the maximum values, which extend from 3.8053 to 6.6827.

According to the hypothesis that the conditions predisposing to landslides are likely to be repeated and based on the values used to construct the success curve, it is possible to affirm that, in an indeterminate period of time, 79.2 % of landslides will occur in class 4, 15.7% – in class 3, 5.0% – in class 2 and 0.1% – in class 1. It can therefore be concluded that class 4 represents areas with very high probability of slippage.

However, it should be emphasized that these values only reflect the susceptibility of risk areas spatially, which differs from the hazard map which also takes into account the temporal probability of occurrence.

4. Assessment of the Robustness and Accuracy of the Model used to Map Susceptibility

4.1. Development of the Success Curve

To assess the reliability of the model used to map the susceptibility of terrains, you can actually create a logarithmic curve by following the process described below:

- Export the informative values (VI) used to construct the susceptibility map from the GIS and place them in a column of a table, sorted in descending order.
- The second column of the table represents the number of pixels assigned to each VI value, while the third column indicates the land area where landslides occurred in those pixels.
- Create a fourth column using the following formula: each cell in this column is the sum of the pixels of the first n cells in the second column, divided by the total pixels. Given that each pixel corresponds to an elementary surface of the study area (10 meters by 10), this column represents the accumulation of surfaces classified in decreasing order of VI, divided by the total surface. The values in this column are therefore all between 0 and 1.
- Create a fifth column in the same way as the fourth but using the values of the land areas where landslides have occurred.
- Construct the success curve using the values in the fourth column on the abscissa and those in the fifth column on the ordinate, using a logarithmic scale.

In summary, this process allows you to create a logarithmic curve that represents the success rate of the model used for terrain susceptibility mapping. This curve is constructed by using the informative values exported from the GIS and by calculating the accumulations of the land surfaces classified in descending order of VI.

The Fig.6 presents the value "AUC", which is the abbreviation of "Area Under the Curve". This value is a measure of the reliability of the model and has no unit. The higher the AUC value, the more robust the model is considered. In general, a value greater than 0.85 indicates a good model for representing susceptibility. In this case, the value of the AUC is 0.86, which constitutes a first element of validation of the model created.

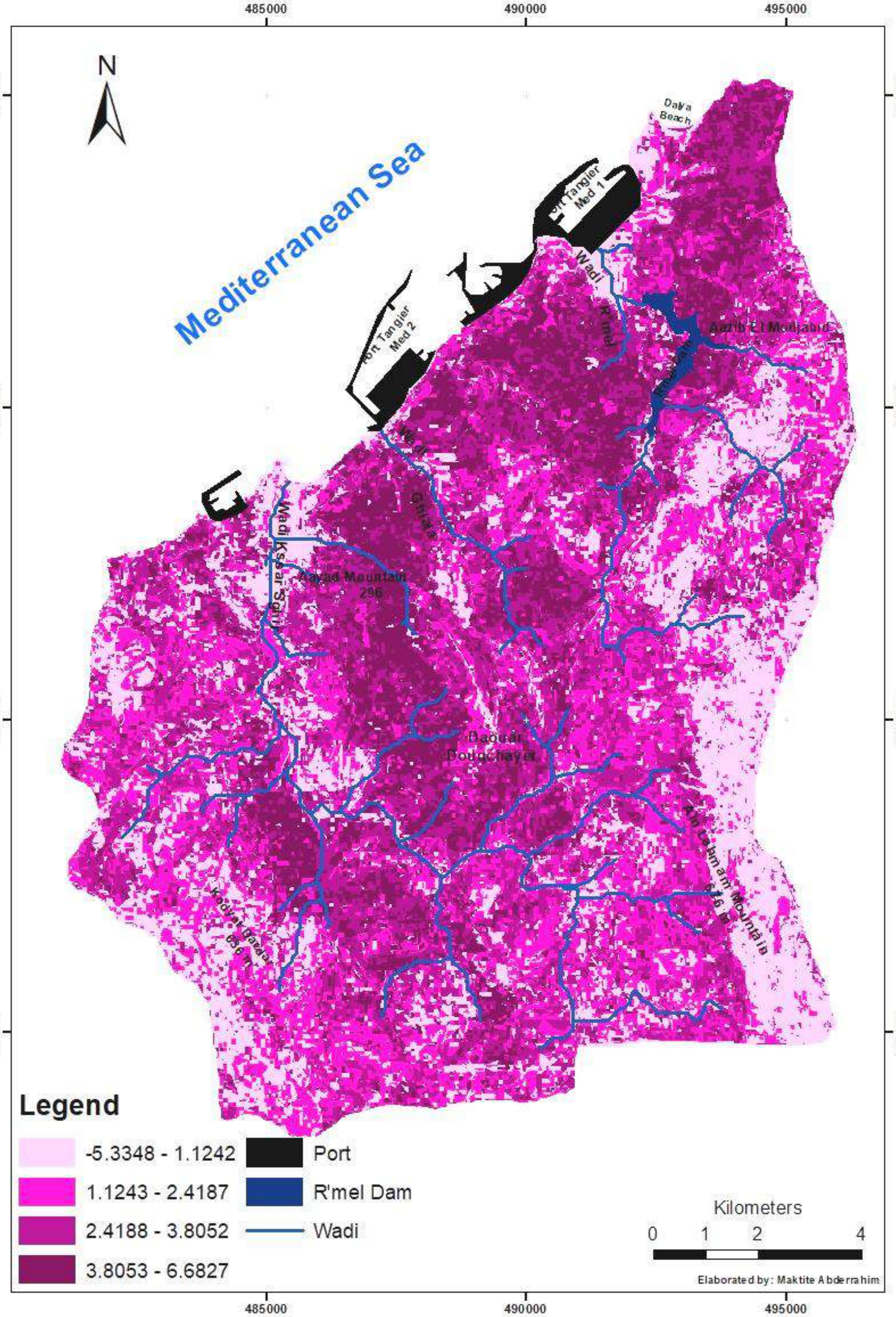

Source: superposition of variables in Fig. 3
Directed by: Maktite Abderrahim

Fig. 5. Susceptibility map of the study area

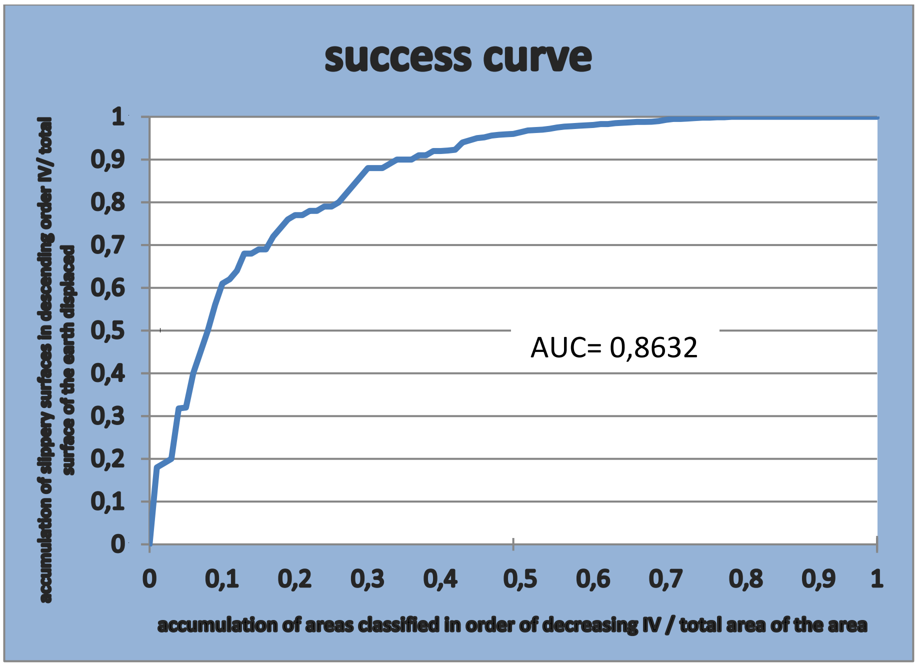

Source: Susceptibility map database

Fig. 6. Success curve

It can be observed on the curve that the value 0.1 on the abscissa axis corresponds to a value of 0.61 on the ordinate axis. This means that the 10% of the surface of the study area that was identified by the model as having the greatest susceptibility contains 61% of the suspected landslides. Additionally, 79% of suspected landslides are in the 25% most likely terrain. These results testify to the reliability of the model, which succeeded in identifying the surfaces most susceptible to slippage. Assuming that, the next slides will take place under conditions similar to the previous ones.

The validity of the constructed model was confirmed using the landslide data that was used to construct it. However, to more accurately assess its accuracy, it would be necessary to introduce another method and to verify whether the model produces comparable results. This principle was used to create the forecast curves.

A common practice is to randomly divide a dataset into two groups in order to construct a forecast curve from a single dataset. The process involves using the first group to develop a susceptibility model, which is then assessed using the second group. This method was used in the case of 277 presumed landslides, where the first group of 124 landslides (land movement cited by: André A. and El Gharbaoui B., 1973) was used to create a susceptibility model. The latter was then validated based on the 153 points of the second group (quoted from Google Earth images). Using this approach, a prediction curve was established (shown in red in Fig. 6) and can be compared to the success curve (in blue in Fig. 5) to assess model performance.

4.2. Development of Forecast Curves

To assess the performance of the susceptibility representation model, two prediction curves were developed in this study.

The first curve was constructed by randomly separating the 277 presumed landslides into two groups. The first group, comprising 124 landslides from the geomorphology map (El Gharbaoui, 1981) and the André Filipe map (table 2), was used to generate the susceptibility map, which should not be confused with the map constructed from all 277 slips. Then, the remaining 153 swipes from the second group were used to validate the same map. A prediction curve was then created using the same methods as for the success curve.

The prediction curves are visually compared to the success curve and their accuracy is assessed by calculating the area under each curve. This analysis makes it possible to assess the accuracy of the susceptibility model and to determine its reliability for predicting new landslides.

4.2.1. Forecast Curve 1

The model used for this validation was developed from the 277 points. The prediction curve 1 obtained (in red in Fig. 6) was compared to the success curve (in blue in Fig. 5).

The prediction and success curves have notable similarities, while their area under the curve (AUC) values is close.

The analysis of the success curve shows that the model is highly effective. Specifically, 10% of the area identified as most likely to experience slips contains 59% of the actual slips, while 25% of the most likely area includes 78.5% of the slips. This indicates that the model is very reliable in predicting where slips will occur.

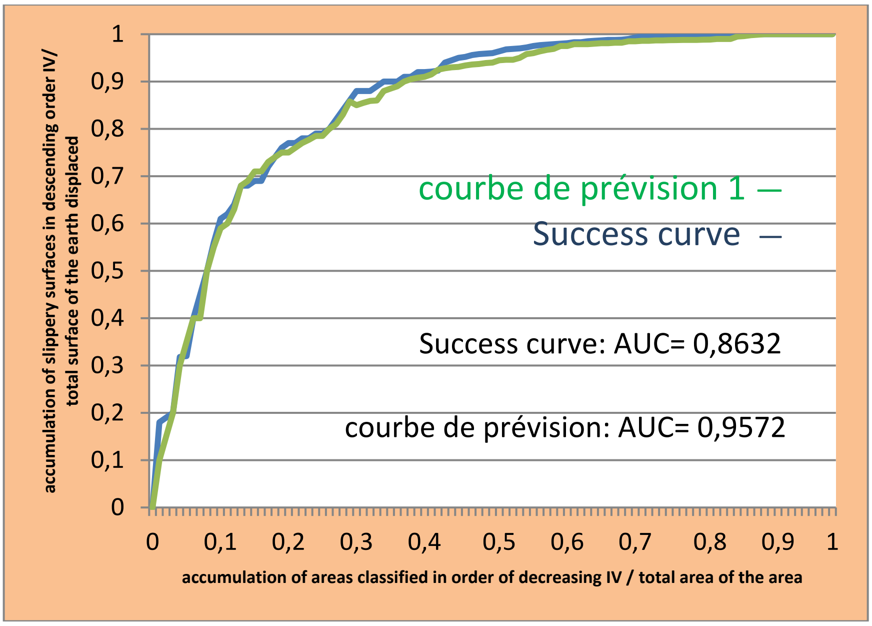

Source: Susceptibility map database

Fig. 7. Forecast curve 1

The prediction curve 1 obtained using the model created from the 124 points is very close to the success curve (Fig. 5). The shape of their plot is similar, and their AUC is higher than that of the success prediction curve, which was 0.8632.

4.2.2. Forecast Curve 2

Nevertheless, the evaluation focused on the resistance of the model developed from the points of group 1. Thus, a second forecast curve was established to evaluate the one created from the 277 potential slips, which were used to establish the susceptibility map of the study area.

The results of forecast curve 2 confirm the accuracy of the model developed, where the most likely 10% of the surface contains 57% of the confirmed landslides and the most likely 25% contains 78% of these landslides. These results demonstrate the effectiveness of the inventory carried out to create a model of land susceptibility. Consequently, the information collected on this area is sufficient to create a fairly accurate terrain susceptibility model.

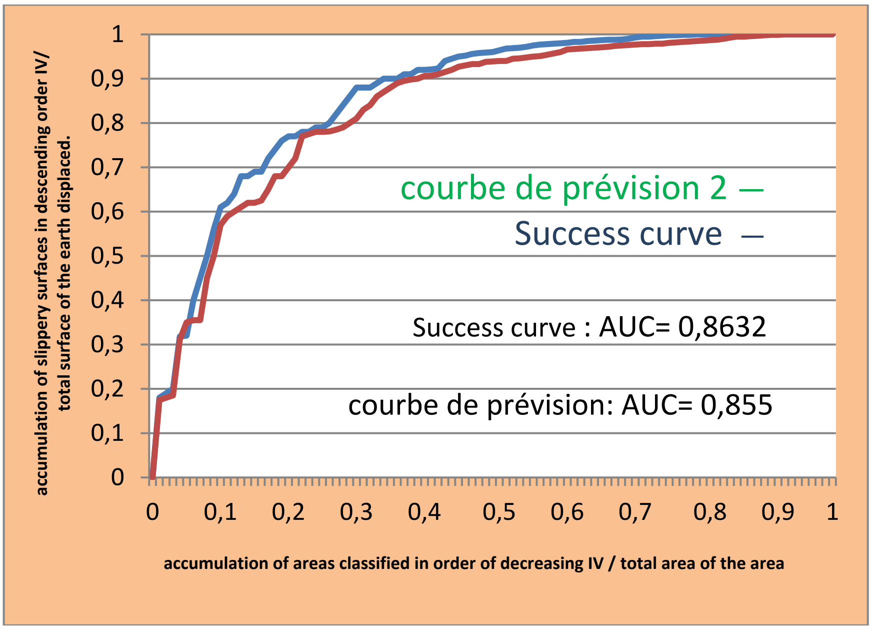

Source: Susceptibility map database

Fig. 8. Forecast curve 2

B. Hazard Map of the Area

The hazard map is generated from the susceptibility map based on the 277 presumed landslides and validated by the success and prediction curves. Each class in the susceptibility map is associated with a probability of temporal occurrence (Zêzere et al., 2004), assuming that the amount of land that will slip in the study area over the next forty years will be similar to that which has slipped in the past forty years. The choice of this forty-year period was motivated by the availability of data from a previous study carried out by El Gharbaoui in 1981, a period marked by heavy rainfall that triggered numerous landslides, thus offering a learning opportunity.

Using this assumption, the estimate of the total area of the area that will experience landslides over the next forty years is obtained by adding the areas of landslides that have occurred in this area over the past forty years. This sum gives a value of 21,973,800 m².

Quantiles were used to distribute the hazard values, creating four classes with approximately equal areas containing an equivalent number of values. However, it is important to note that the number of pixels in each class may vary slightly due to the grouping of pixels with similar values in the same class. The probability P for each class was calculated using the x and y coordinates of the success curve, which helps to determine the probability of a slip occurring in a pixel belonging to a given class over the next 40 years. For example, class 3 has a probability of 0.017, which means that there is a 1 in 59 chance of experiencing landslide within the next forty years (as shown in Table 3).

Thus, the hazard map presented indicates the probability of occurrence of a landslide for each pixel of the study area over the next forty years.

The hazard map is based on the susceptibility map of the studied area (Zêzere et al., 2008), which was presented previously. However, the hazard map differs from the susceptibility map because it incorporates not only the spatial susceptibility, but also the temporal probability of landslide for each pixel over the next forty years. The values obtained make it possible to assess the severity of the hazard according to the probability of a landslide. The results are presented in Table 4 and will be used to generate the risk map.

C. Vulnerability Map

Research on landslide vulnerability on a global scale is limited, which makes the assessment method proposed in this study rather forward-looking and potentially in need of further study. However, this method allows an overall assessment of the vulnerability of an area, as well as its impact on the representation of risk.

The study of the vulnerability of the study area was based on two main criteria: the first is the criterion of bodily harm, which includes a population index and a road use index (Tables 5 and 6), while the second is the structural damage criterion, which includes a population density index and a road damage index (Tables 7 and 8).

Table 3

Values of the probability of temporal occurrence obtained by equation (2)

Hazard classes	**Surface m²**	**Contact details**		**$P_r = y_i - y_{i-1}$**	**Probability P**	**Chance of slipping in 40 years**
		x	y			
1	48437165	0.25	0.79	0.79	0.358	1⁄3
2	48375733	0.50	0.96	0.17	0.077	1⁄13
3	48585329	0.75	0.997	0.037	0.017	1⁄59
4	48288816	1	1	0.003	0.0014	1⁄714

Table 4

Qualification of hazard classes

Class	Probability	Chance of experiencing slippage in 40 years	Hazard
1	0.358	One in 3	Very weak
2	0.077	One in 13	Weak
3	0.017	One in 59	Strong
4	0.0014	One in 714	Very strong

The global vulnerability map was developed based on two separate maps assessing structural damage and bodily harm. To build these maps, loss index values were assigned to different elements at risk. For each pixel, the sum of the loss indices of these different elements was calculated, then the results were normalized on a scale of 0 to 1 to represent the vulnerability. A value of 1 corresponds to areas most likely to sustain significant damage.

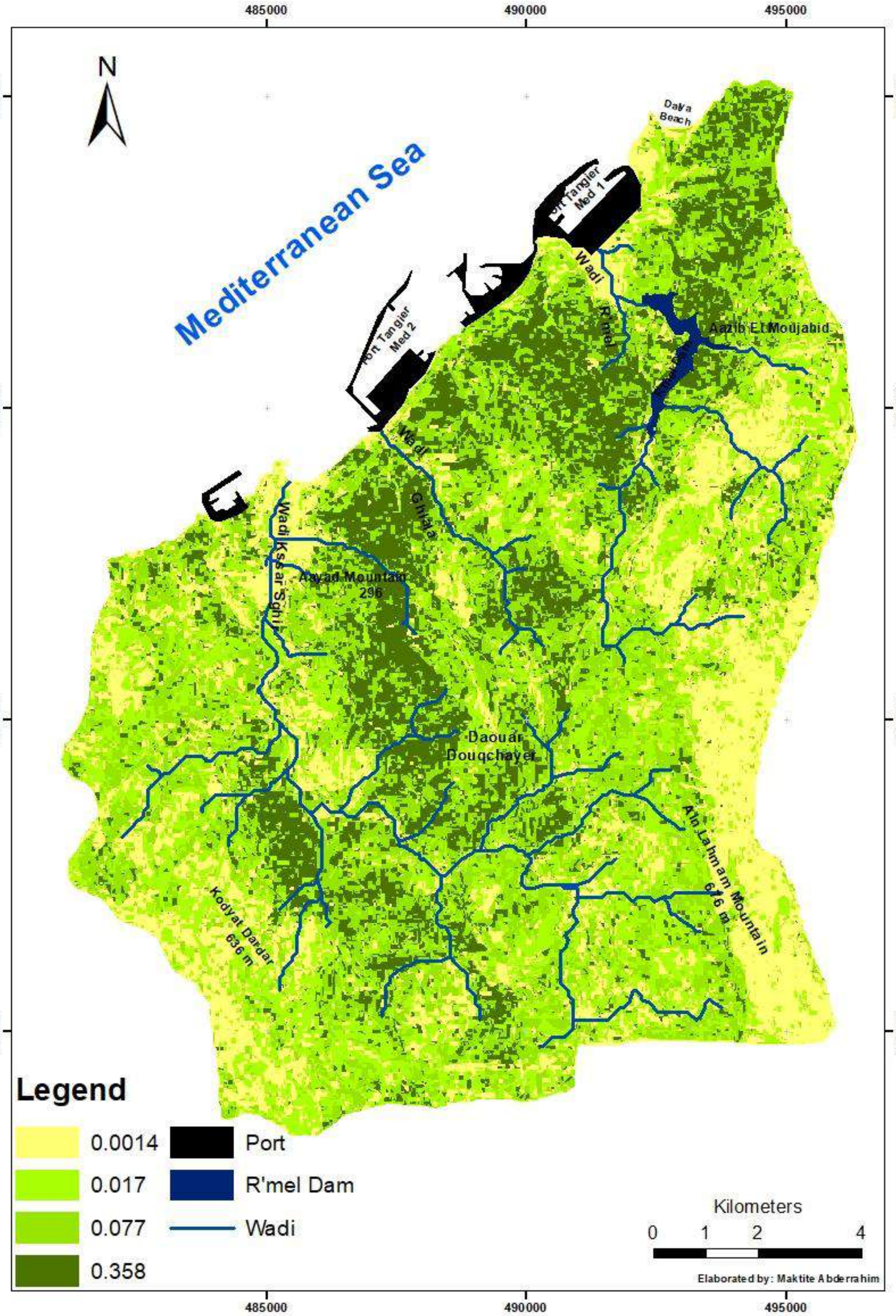

Source: Susceptibility map database
Directed by: Maktite Abderrahim

Fig. 9. Hazard map of the study area

Table 5

Risk index related to road use

Type of roads	Number of users	IV value
National Road N16	**5230**	**1**
A4 motorway	**5003**	**0.957**
Regional Road P4701	**2554**	**0.488**
Regional Road P4613	**1962**	**0.375**
Regional Road P4703	**1700**	**0.325**
Road Walking	**Between 5 and 30**	**0.001 – 0.006**
Railway	**4**	**0.001**

Source: fieldwork + DRETL

Table 6

Risk index linked to the number of populations

Regions	Number of habitats	IV value	Regions	Number of habitats	IV value
AIN CHOUKA	510	0.27	ANASSAR	512	0.28
AIN LAAKAYZ	177	0.09	MANSOURA	466	0.25
OUED GHLALA	545	0.29	ELHAMA	209	0.11
AIN RMEL	989	0.53	ZHARA	404	0.22
BOUAAYAD	1355	0.73	ELGHOUJIN	991	0.53
DALYA	267	0.14	HTATECH	242	0.13
DCHER BIN LWIDAN	1075	0.58	KSSER LMAJAZ CENTER	927	0.50
DHER LGHAROUB	1856	1	KSSER SGHIR	490	0.26
LACHBA	753	0.41	MLICH	1075	0.58
DKCHER	614	0.33	OUED RMEL	260	0.14
DCHICHA	488	0.26	TAGHREMT	475	0.26

Source: 2014 census

Table 7

Risk index linked to the density of habitats

Municipality or city	Habitat density index	Municipality or city	Habitat density index
Ksser Sghir	1	Melloussa	0.624
Anjra	0.904	Alain	0.314
Ksser lmajaz	0.669	Taghremt	0.309

Source: 2014 census

Table 8

Risk index linked to the number of ground movements

Type of roads	Landslide inventory	IV value
Regional Road P4701	**23**	**1**
Regional Road P4703	**15**	**0.652**
Regional Road P4613	**14**	**0.609**
National Road N16	**9**	**0.391**
Road Walking	**Between 1 and 3**	**0.130 – 0.043**
A4 motorway	**0**	**0**
Railway	**0**	**0**

Source: fieldwork

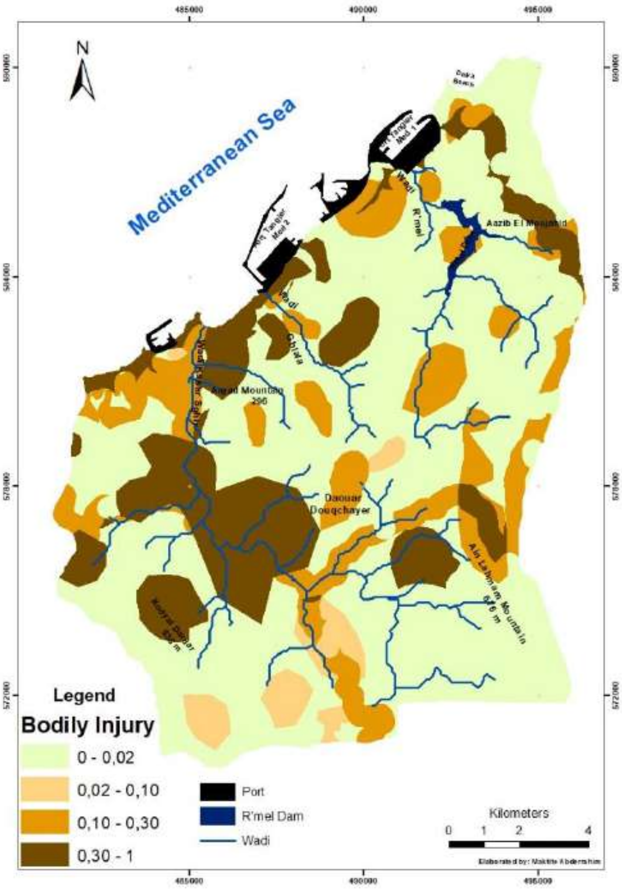

Fig. 10. Bodily injury map

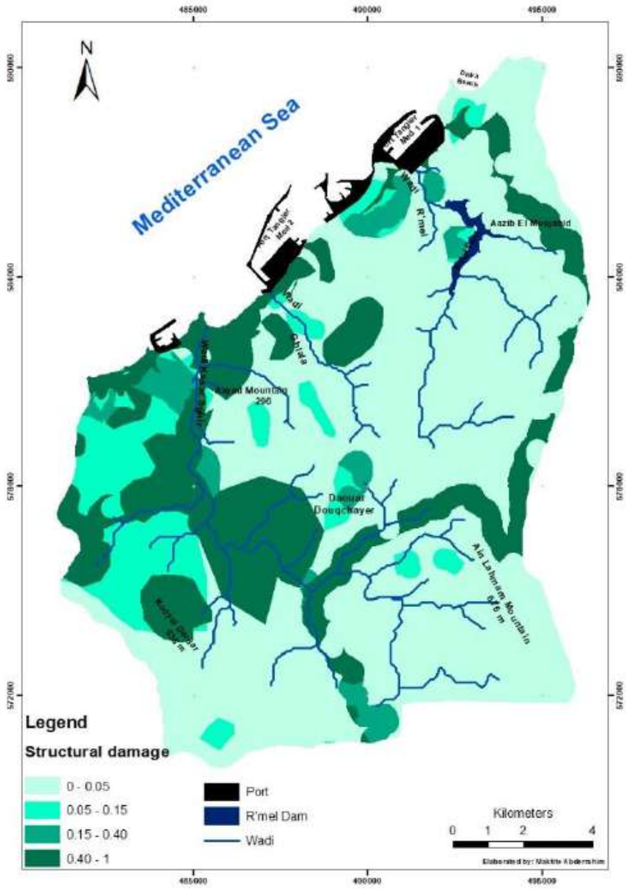

Source: field work + census 2014
Directed by: Maktite Abderrahim

Fig. 11. Structural damage map

Body and structural vulnerability maps have significant similarities due to the risk elements taken into account when developing them. Areas where there is a significant concentration of at-risk elements such as inhabitants, Douars and roads display a higher vulnerability compared to areas where these elements are less present. In addition, there is a correlation between certain forms of vulnerability for certain elements at risk, especially for roads, where bodily and structural vulnerabilities are high.

The vulnerability values have been divided into four classes separated into quantiles, in the same way as for the susceptibility of the terrain or for the hazard. The results, shown in Table 9, were used to create the risk map.

By examining Figs 9 and 12, it can be seen that the areas with very high vulnerability are mainly found in the northern part of the study area, while the land exposed to a strong hazard is located in the northern half near the port and forest projects. This suggests that the inhabitants have not developed a certain awareness of the risks, choosing to settle in areas where the hazard is higher.

D. Risk Map

Quantiles of hazard and vulnerability classes have been established (see Tables 4 and 9). The risk is then assessed by crossing these hazard and vulnerability classes (see Table 1).

The risk map results from the combination of the hazard and vulnerability maps. The areas most at risk are mainly located in the northern half of the study area, which corresponds to the most vulnerable area.

Table 9

Qualification of vulnerability classes

Classes	Loss index value	Vulnerability
1	From 0 to 0.24	**very low**
2	From 0.25 to 0.30	**Weak**
3	From 0.31 to 0.36	**Strong**
4	From 0.37 to 1	**Very strong**

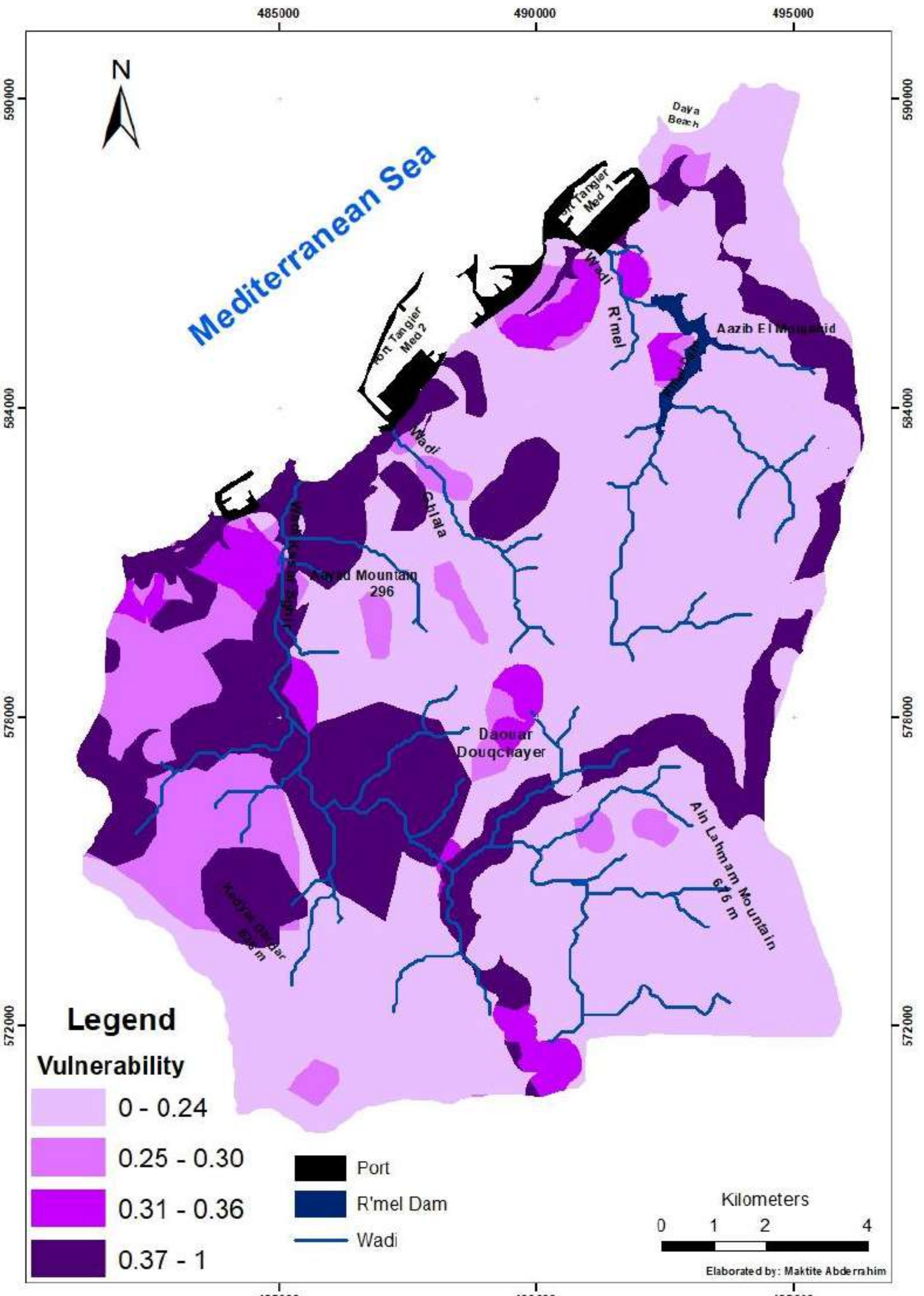

Source: Overlay of maps Figs 10 and 11
Directed by: Maktite Abderrahim

Fig. 12. Vulnerability map of the study area

Table 10

Qualification of risk classes

Classes	Risk index value	Type of risk
1	From 0 to 0.24	Very weak
2	From 0.25 to 0.30	Weak
3	From 0.31 to 0.36	Strong
4	From 0.37 to 1	Very strong

Source: Description of the method
Directed by: Maktite Abderrahim

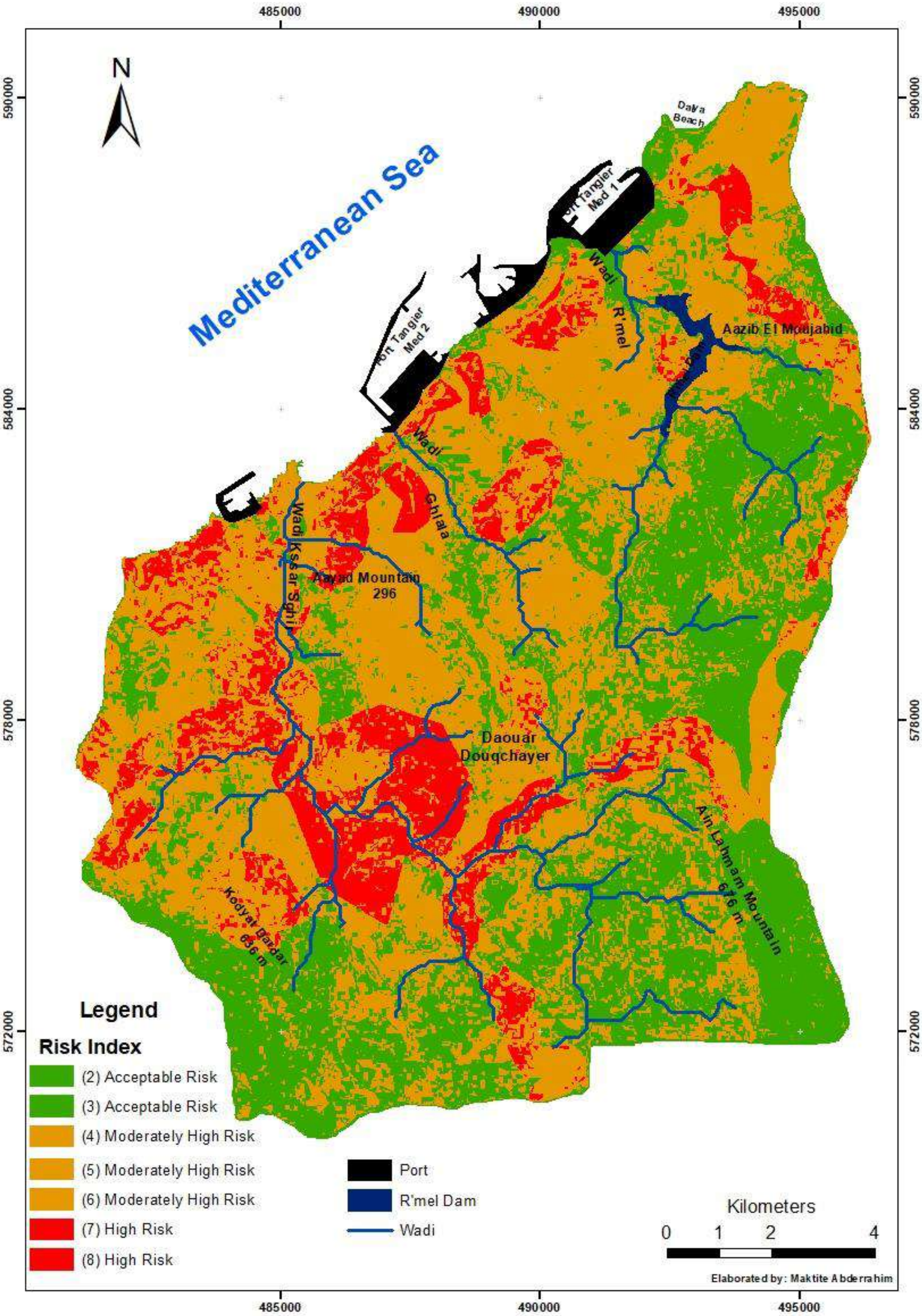

Source: overlay of maps Figs 9 and 12
Directed by: Maktite Abderrahim

Fig. 13. Landslide risk map

Although the accuracy of the susceptibility map was confirmed by the success and prediction rates, the validity of the risk map can be questioned as it was developed from the vulnerability map which requires study with a more in-depth methodology. Additionally, the vulnerability map only considers risk items for which data are available, which may affect the accuracy of the risk map.

In order to ensure effective land use planning, regions presenting a high risk will require the implementation of prevention and protection measures. One of the most important preventive measures is to prohibit construction in high-hazard areas. Drainage can be used to prevent slope erosion, while reforestation can reduce the impact of water on soils. Excavating the top of rotational landslides can help stabilize these areas, while building retaining walls along roads can retain soils.

For areas with moderately high risk, it is essential to design them in such a way that they do not increase the existing risk. Prevention and protection measures can also be put in place to reduce the level of risk and bring it down to an acceptable level, thus ensuring a more secure development.

IV. Conclusion

The objective of this study is to develop methods for assessing the hazard and risk associated with landslides using a common conceptual model. This method made it possible to generate a susceptibility map for the study area, as well as hazard, vulnerability and risk maps associated with this same area. The resolution of the Digital Terrain Model (DTM) used for this study was 10 meters, which provided detailed results for in-depth regional analysis. The evaluation of the quality of the susceptibility model was carried out using success and prediction curves, thus demonstrating the reliability and accuracy of the method employed.

The hazard map was developed based on the assumption that the amount of land that will slip in the study area over the next forty years will be similar to that which has slipped in the same area over the past forty years. This hypothesis is interesting because it only requires information on the area of the landslides and their approximate date to calculate the temporal probability of occurrence of the landslides, thus making it possible to obtain the hazard map.

By crossing the hazard and vulnerability maps, a risk map was generated. The method developed in this study is promising because it allows obtaining significant results with a relatively small volume of data. This represents a considerable advantage for its application in the Regional Development Plans.

REFERENCES

Avenard J.M. The current erosion in the Sebou basin. Report of the National Institute of Agricultural Research (INRA). Rabat, 1965, 114 p. (in French).

André A. and El Gharbaoui A. Aspects of the coastal morphology of the Tangier peninsula. Journal of the Geography of Morocco, No. 23-24, 1973, pp. 125-149 (in French).

Brabb E.E. Innovative approaches to landslide hazard mapping. Proceed. IV lnt. Symp. Landslides, Toronto, Vol. 1, 1984, pp. 307-324.

Brabb E.E. Analyzing and portraying geologic and cartographic information for land-use planning, emergency response, and decision making in San Mateo County, California. Proc. GIS'78, San Fransisco, ll-nd Annual Int. Conf. on GIS, 1987, pp. 362-374.

Brabb E.E. The San Mateo County GIS project for predicting the consequences of hazardous geologic processes. In: Geographical information system in assessing natural hazards (Carrara A. and Guzzetti F., eds.). Kluwer Academic Publishers. Dordrecht, 1995, pp. 299-334.

Carrara A., Cardinali M., Guzzetti F., Reichenbach P. GIS-based techniques for mapping landslide hazard. In: Geographical information system in assessing natural hazard (Carrara A. and Guzzetti F., eds.), Kluwer Acad. Publ. Dordrecht, 1995, pp. 135-176.

Chung C.F. and Fabbri A. Validation of spatial prediction models for landslide hazard mapping. Natural Hazards, Vol. 30, 2003, pp. 451-472, https://doi.org/10.1023/B:NHAZ.0000007172.62651.2b.

Dai F.C., Lee C.F., Ngai Y.Y. Landslide risk assessment and management: an overview. Engineering Geology, Vol. 64, No. 1, 2002, pp. 65-87, https://doi.org/10.1016/S0013-7952(01)00093-X.

El Gharbaoui A. Earth and man in the Tingitan Peninsula. Essay on man and the natural environment in the Western Rif. Work of the Scientific Institute, Geology and Physical Geography Series, No. 15, 1981, Rabat (in French).

El Kharim Y. Study of slope movements in the Tetouan region (Western Rif): Inventory, analysis and mapping. PhD thesis Es-Sciences, Abdelmalek Essaadi University, Tetouan, Morocco, 2002, 250 pp. (in French).

REFERENCE

Avenard J.M. L'érosion actuelle dans le bassin de Sebou. Rapport de l'institut national de recherche Agronomique (INRA). Rabat, 1965, 114 p.

Andre A. et El Gharbaoui A. Aspects de la morphologie littorale de la péninsule de Tanger. Revue de la Géographie du Maroc, No. 23-24, 1973, pp. 125-149.

Brabb E.E. Innovative approaches to landslide hazard mapping. Proceed. IV lnt. Symp. Landslides, Toronto, Vol. 1, 1984, pp. 307-324.

Brabb E.E. Analyzing and portraying geologic and cartographic information for land-use planning, emergency response, and decision making in San Mateo County, California. Proc. GIS'78, San Fransisco, ll-nd Annual Int. Conf on GIS, 1987, pp. 362-374.

Brabb E.E. The San Mateo County GIS project for predicting the consequences of hazardous geologic processes. In: Geographical information system in assessing natural hazards (Carrara A. and Guzzetti F., eds.). Kluwer Academic Publishers. Dordrecht, 1995, pp. 299-334.

Carrara A., Cardinali M., Guzzetti F., Reichenbach P. GIS-based techniques for mapping landslide hazard. In: Geographical information system in assessing natural hazard (Carrara A. and Guzzetti F., eds.), Kluwer Acad. Publ. Dordrecht, 1995, pp. 135-176.

Chung C.F. and Fabbri A. Validation of spatial prediction models for landslide hazard mapping. Natural Hazards, Vol. 30, 2003, pp. 451-472, https://doi.org/10.1023/B:NHAZ.0000007172.62651.2b.

Dai F.C., Lee C.F., Ngai Y.Y. Landslide risk assessment and management: an overview. Engineering Geology, Vol. 64, No. 1, 2002, pp. 65-87, https://doi.org/10.1016/S0013-7952(01)00093-X.

El Gharbaoui A. La Terre et l'Homme dans la Péninsule Tingitane. Essai sur l'Homme et le milieu naturel dans le Rif occidental. Travaux de l'Institut Scientifique, Série géologie et géographie physique, No. 15, 1981, Rabat.

El Kharim Y. Etude des mouvements de versants dans la région de Tétouan (Rif occidental): Inventaire, analyse et cartographie. Thèse de Doctorat Es-Sciences, Université Abdelmalek Essaadi, Tétouan. Maroc, 2002, 250 p.

Faleh A., Sadiki A., Haloui B., Akdim B. Application of mineralogical and geotechnical analyses of clays in the study of landslides: examples from the Central Prerif (northern Morocco). Geography Papers, No. 35, January-June, 2002, pp. 115-128, Spain (in Spanish).

Fares A., Rollet M., Broquet P. Methodology for mapping natural hazards related to ground movements. French Journal of Geotechnics, No. 69, 1994, pp. 63-72 (in French).

Flageollet J-C. Field movements and their prevention. Geographical Collection. Paris, Masson, 1989, 224 p. (in French).

Fofana O. Preparation of a landslide risk map of the Kser SGHIR area (northern Rif, Morocco). Final thesis for the Diploma of State Engineer in Agronomy. Institute of Agronomy and Veterinary Medicine Hassan II, 2009 (in French).

Fonseca André Filipe. Large deep-seated landslides in the northern Rif Mountains (Northern Morocco): inventory and analysis. Doctoral thesis, 2014.

Hansen A. Landsat hasard analysis. In: Slope instability (Brunsden D. et Prior D.B., eds.). John Wiley ans Sons. Chichester, 1984, pp. 523-602.

Irigaray C. Hillside movements: Inventory, analysis and susceptibility mapping using a Geographic Information System. Application to the areas of Colmenar (Malaga), Rute (Córdoba) and Montefrio (Granada). PhD thesis, Granada University, 1995, 384 p. (in Spanish).

Leone F. Concept of vulnerability applied to the assessment of the risks generated by field movements. Orleans. BRGM, Doctoral thesis, 1996 (in French).

Leroi E., Rouzeau O., Scanvic J.Y., Weber C.C, Vergas-Curvo G. Remote sensing landslide hazard mapping using GIS technology in Colombia Andes. Episode, Vol. 15, No. 1, 1992, pp. 32-35, DOI:10.18814/epiiugs/1992/v15i1/006.

Maate A. Alpine paleogeographic stratigraphy and evolution of the Gomaride domain (internal Rif, Morocco). Doctoral thesis, University of Granada, Department of Stratigraphy and Paleontology, Spain, 1996, 397 p., http://hdl.handle.net/10481/53657 (in Spanish).

Margaa Kh. Natural hazards mapping test: application to the development of the Al Hoceima region (Rif, northern Morocco). PhD thesis, University of Franche-Comté, 1994, 196 p., Corpus ID: 127852669 (in French).

Maquaire O., Ambrose B. Geomorphological hazards (ground movements) – process, operation, maps. Strasbourg: s.n, 2002.

Milliès-Lacroix A. Landslides. Presentation of a forecast map of mass movements in the Rif (northern Morocco). Mining and Geology, Vol. 27, 1968, pp. 43-53 (in French).

Rouzeau O. and Scanvic J.Y. Use of satellite data for the study of ground movements and the production of susceptibility maps. Géo Observateur, No. special, Marisy 92, Rabat, 1992, pp. 265-270 (in French).

Soeters R. and van Westen C.J. Slope instability recognition, analysis and zonation. In: Landslides: Investigation and Mitigation (Turner A.K., Schuster R.L., éds.), Transportation Research Board, National research Council, Special report 247, National Academy Press. Washington D.C., USA, 1996, pp. 129-177.

Sossey A. Processing and integration of optical and radar satellite data in a GIS with a view to obtaining a map of the hazard linked to the instability of the terrain in the Tangier peninsula (northern Rif, Morocco). PhD, Mohamed V University, Faculty of Sciences, Rabat, 2005, 175 p. (in French).

UNDRO (Office of the United Nations Disaster Relief Coordinator). Natural disasters and vulnerability analysis. Report of Expert Group Meeting, 1979, 19 p.

van Westen C.J. Remote sensing and geographic information systems for geologic hazard mitigation. ITC Journal, No. 4, 1993, pp. 393-399.

Faleh A., Sadiki A., Haloui B., Akdim B. Application des analyses minéralogique et géotechniques des argiles dans l'étude des glissements de terrains: exemples du Prérif central (Maroc septentrional). Papeles de Geografía, No. 35, enero-junio, 2002, pp. 115-128, España.

Fares A., Rollet M., Broquet P. Méthodologie de la cartographie des risques naturels liés aux mouvements de terrain. Revue Française de Géotechnique, No. 69, 1994, pp. 63-72.

Flageollet J-C. Les mouvements de Terrain et leur prévention. Collection Géographique. Paris, Masson, 1989, 224 p.

Fofana O. Elaboration d'une carte de Risque de Glissement de terrain de la zone de Kser SGHIR (Rif septentrional, Maroc). Mémoire de fin d'étude pour l'obtention du Diplôme d'ingénieur d'Etat en Agronomie. Institut Agronomique Et Vétérinaire Hassan II, 2009.

Fonseca André Filipe. Large deep-seated landslides in the northern Rif Mountains (Northern Morocco): inventory and analysis. Doctoral thesis, 2014.

Hansen A. Landsat hasard analysis. In: Slope instability (Brunsden D. et Prior D.B., eds.). Chichester. John Wiley ans Sons. 1984, pp. 523-602.

Irigaray C. Movimientos de ladera: Inventario, analisis y cartografia de susceptibilidad mediante un Systema de Informaciôn Geografica. Aplicacion a las zonas de Colmenar (Malaga), Rute (Cordoba) y Montefrio (Granada). Thèse de Doctorat, Université de Granada, 1995, 384 p.

Leone F. Concept de vulnérabilité appliquée à l'évaluation des risques générés par les phénomènes de mouvements de terrain. Orléans. BRGM, Thèse de doctorat, 1996.

Leroi E., Rouzeau O., Scanvic J.Y., Weber C.C, Vergas-Curvo G. Remote sensing landslide hazard mapping using GIS technology in Colombia Andes. Episode, Vol. 15, No. 1, 1992, pp. 32-35, DOI:10.18814/epiiugs/1992/v15i1/006.

Maate A. Estratigrafía y evolución paleogeográfica alpina del dominio gomáride (Rif interno, Marruecos). Tesis doctoral, Universidad de Granada, Departamento de Estratigrafía y Paleontología, España, 1996, p 397, http://hdl.handle.net/10481/53657.

Margaa Kh. Essai de cartographie des risques naturels: application à l'aménagement de la région d'Al Hoceima (Rif, Nord-Maroc). Thèse Doctorat, Université de Franche-Comté, 1994, 196 p., Corpus ID: 127852669.

Maquaire O., Ambroise B. Aléas géomorphologiques (mouvements de terrains) –processus, fonctionnement, cartographies. Strasbourg: s.n, 2002.

Milliès-Lacroix, A. Les glissements de terrain. Présentation d'une carte prévisionnelle des mouvements de masse dans le Rif (Maroc septentrional). Mines et Géologie, 27, 1968, pp. 43-53.

Rouzeau O. et Scanvic J.Y. Utilisation des données satellitaires pour l'étude des mouvements de terrain et la réalisation de cartes de susceptibilité. Géo Observateur, No. spécial, Marisy 92, Rabat, 1992, pp. 265-270.

Soeters R. and van Westen C.J. Slope instability recognition, analysis and zonation. In: Landslides: Investigation and Mitigation (Turner A.K., Schuster R.L., éds.), Transportation Research Board, National research Council, Special report 247, National Academy Press. Washington D.C., USA, 1996, pp. 129-177.

Sossey A. Traitement et intégration des données satellitaires optiques et Radar dans un SIG en vue de l'obtention de carte de l'aléa lié aux instabilités de terrain dans la péninsule de Tanger (Rif septentrional, Maroc). Doctorat, Université Mohamed V, Faculté des Sciences, Rabat. 2005, 175 p.

UNDRO (Office of the United Nations Disaster Relief Coordinator). Natural disasters and vulnerability analysis. Report of Expert Group Meeting, 1979, 19 p.

van Westen C.J. Remote sensing and geographic information systems for geologic hazard mitigation. ITC Journal, No. 4, 1993, pp. 393-399.

van Westen C.J., van Duren I., Kruse H.M.G., Terlien M.T.J. GISSIZ: training package for Geographic Information Systems in slope instability zonation. ITC-Publication Number 15, ITC, Enschede, The Netherlands. Volume 1 – Theory, 245 pp., Volume 2 – Exercises, 1993, 359 pp.

Wadge G. The potential for volcanic disaster in the Lesser Antilles arc. Bulletin of Volcanology, Vol. 50(2), 1988, pp. 198-215.

Yin K.L. and Yan T.Z. Statistical prediction model for slope instability of metamorphosed rocks. Proceeding 5th International Symposium on Landslides, Lausanne, Switzerland, Vol. 2, 1988, pp.1269-1272.

Zêzere J.L., Garcia RAC., Oliveira SC, Reis E. Probabilistic Landslide risk analysis considering direct costs in the area north of Lisbon (Portugal). Geomorphology, Elsevies. Vol. 94, 2008, pp. 467-495.

Zêzere J.L., Reis E., Garcia R., Oliveira S., Rodrigues M.L., Vieira G., Ferreira A.B. Integration of spatial and temporal data for the definition of different landslide hazard scenarios in the area north of Lisbon (Portugal). Natural hazards and Earth system Sciences, European Geosciences Union, Vol. 4, 2004, pp.133-146, https://doi.org/10.5194/nhess-4-133-2004.

van Westen C.J., van Duren I., Kruse H.M.G., Terlien M.T.J. GISSIZ: training package for Geographic Information Systems in slope instability zonation. ITC-Publication Number 15, ITC, Enschede, The Netherlands. Volume 1 – Theory, 245 pp., Volume 2 – Exercises, 1993, 359 pp.

Wadge G. The potential for volcanic disaster in the Lesser Antilles arc. Bulletin of Volcanology, Vol. 50(2), 1988, pp. 198-215.

Yin K.L. and Yan T.Z. Statistical prediction model for slope instability of metamorphosed rocks. Proceeding 5th International Symposium on Landslides, Lausanne, Switzerland, Vol. 2, 1988, pp. 1269-1272.

Zêzere J.L., Garcia RAC., Oliveira SC, Reis E. Probabilistic Landslide risk analysis considering direct costs in the area north of Lisbon (Portugal). Geomorphology, Elsevies. Vol. 94, 2008, pp. 467-495.

Zêzere J.L., Reis E., Garcia R., Oliveira S., Rodrigues M.L., Vieira G., Ferreira A.B. Integration of spatial and temporal data for the definition of different landslide hazard scenarios in the area north of Lisbon (Portugal). Natural hazards and Earth system Sciences, European Geosciences Union, Vol. 4, 2004, pp.133-146, https://doi.org/10.5194/nhess-4-133-2004.

МОДЕЛИРОВАНИЕ ОПОЛЗНЕЙ, ОБРАЗУЮЩИХСЯ В ВЕРХНЕЙ ЧАСТИ ПОРТА ТАНЖЕР-МЕД (ТАНЖЕР, МАРОККО), С ИСПОЛЬЗОВАНИЕМ ГИС И СТАТИСТИЧЕСКОГО МЕТОДА

Мактит А., Фалех А.

Факультет литературы и гуманитарных наук, Саис-Фес, кафедра географии,
Университет Сиди Мохаммед бен Абделла, Фес, Марокко

Резюме. Данное исследование имеет решающее значение для понимания проблем, с которыми сталкивается порт Танжер-Мед – стратегический узел международной торговли. Расположенный в горном регионе, этот порт очень уязвим для стихийных бедствий, особенно оползней. Нужно подчеркнуть, что с учетом полученных данных, исследование, проведенное на испытательном полигоне площадью 193 км², зафиксировало 277 движений по склону, что составляет около 11% от общей площади. При оценке восприимчивости местности использовался метод информационной ценности для картирования перемещений за последние десятилетия, а также шесть предрасполагающих к ним факторов.

Результаты показывают, что почти 31% общей площади очень восприимчивы к массовым движениям, 22% очень чувствительны, а 23,3% представляют малую угрозу. Эти результаты были сопоставлены и подтверждены с использованием успешных показателей и кривых прогнозирования. Кроме того, надо отметить, что было выделено пять основных классов риска оползней на неосвоенных или малоосвоенных территориях с низким или незначительным значением риска и на освоенных территориях горных склонов с очень высоким его значением.

Таким образом, точное картирование и анализ рисков необходимы для разработки стратегий управления и предотвращения оползней с целью минимизации потенциального воздействия на портовую инфраструктуру и связанную с ней экономическую деятельность. В заключение можно сказать, что данное исследование способствует лучшему пониманию геологических рисков в регионе и, что более важно, реализации соответствующих мер по обеспечению безопасности и устойчивости порта.

Ключевые слова: *порт, Средиземноморский Танжер, информативность, кривые успешности, кривые прогноза*

QGT VƏ STATİSTİK METODDAN İSTİFADƏ EDİLMƏKLƏ, TANJER-MED LİMANININ (TANJER, MƏRAKEŞ) YUXARI HİSSƏSİNDƏ ƏMƏLƏ GƏLMİŞ SÜRÜŞMƏLƏRİN MODELLƏŞDİRİLMƏSİ

Maktit A., Faleh A.

Ədəbiyyat və humanitar elmlər fakültəsi, Sais-Fes, coğrafiya kafedrası,
Sidi Moxammed ben Abdella Universiteti, Fes, Marakeş

Xülasə. Bu tədqiqat, beynəlxalq ticarətin strateji mərkəzi olan Tanca-Med portunun qarşılaşdığı problemlərin başa düşülməsi üçün həlledici əhəmiyyət daşıyır. Dağlıq bir bölgədə yerləşən bu port, təbii fəlakətlərə, xüsusilə sürüşmələrə qarşı çox həssasdır. 193 km² sahəsi olan sınaq poliqonunda aparılan tədqiqat, ümumi sahənin təxminən 11%-ni təşkil edən 277 yamac hərəkətini qeydə almışdır. Əlavə olaraq, qeyd etmək lazımdır ki, ərazinin həssaslığının qiymətləndirilməsində son onilliklərdə baş vermiş yerdəyişmələri xəritələşdirmək üçün məlumatın qiyməti metodu və onlara səbəb olan altı amildən istifadə edilmişdir. Bundan əlavə əldə edilən nəticələr göstərir ki, ümumi sahənin təxminən 31%-i kütləvi hərəkətlərə çox həssasdır, 22%-i isə yüksək dərəcədə həssasdır və 23,3%-i az risk daşıyır. Həmçinin bu nəticələr uğurlu göstəricilər və proqnozlaşdırma əyrilərindən istifadə edilərək təsdiq edilmişdir. Aşağı və ya əhəmiyyətsiz risk dərəcəsi olan inkişaf etməmiş və ya az inkişaf etmiş ərazilər və yüksək risk dərəcəsi olan dağ yamaclarında yerləşən inkişaf etmiş ərazilər üzrə beş əsas sürüşmə riski sinfi müəyyən edilmişdir. Port infrastrukturuna və ona bağlı iqtisadi fəaliyyətə potensial təsiri azaltmaq məqsədi ilə sürüşmələrin idarə olunması və qarşısının alınması üçün dəqiq xəritələşdirmə və risklərin təhlili vacibdir. Nəticə etibarilə, bu tədqiqat regiondakı geoloji risklərin daha yaxşı başa düşülməsinə və daha da əhəmiyyətlisi, port təhlükəsizliyi və davamlılığını təmin etmək üçün müvafiq tədbirlərin həyata keçirilməsinə töhfə verir.

Açar sözlər: *port, Tanca Aralıq dənizi, məlumatlılıq,uğurluq əyriləri, proqnoz əyriləri*